

# Microwave transport approach to the coherence of interchain hopping in $(\text{TMTSF})_2\text{PF}_6$

P. Fertey<sup>1,a</sup>, M. Poirier<sup>1</sup>, and P. Batail<sup>2</sup>

<sup>1</sup> Centre de Recherche en Physique du Solide, Département de Physique, Université de Sherbrooke, Sherbrooke, Québec, Canada J1K 2R1

<sup>2</sup> Institut National des Matériaux de Nantes, 2 rue de la Houssinière, BP 32229, 44322 Nantes Cedex 3, France

Received 27 January 1999

**Abstract.** We report a microwave study of the longitudinal and transverse transport properties of the quasi-one-dimensional organic conductor  $(\text{TMTSF})_2\text{PF}_6$  in its normal phase. The contactless technique have provided a direct measurement of the temperature profile of the resistivity along the  $\mathbf{b}'$  direction and in magnetic fields up to 14 T. A characteristic energy scale ( $T_x \sim 40$  K) has been observed which delimits a transient regime from an insulating to a metallic behavior. This anomalous profile is discussed in terms of the onset of coherent transport properties along the  $\mathbf{b}'$  direction below 40 K. This is also supported by the observation of a finite longitudinal and transverse magnetoresistances only below 40 K, indicative of a two-dimensional regime. Below  $T_x$ , however, strong deviations with respect to a Fermi liquid behavior are evidenced.

**PACS.** 67.55.Hc Transport properties – 71.27.+a Strongly correlated electron systems, heavy fermions – 71.10.Pm Fermions in reduced dimensions (anyons, composite fermions, Luttinger liquid, etc.)

## 1 Introduction

Due to a pronounced chain structure, the  $(\text{TMTSF})_2\text{X}$ , [X =  $\text{PF}_6$ ,  $\text{AsF}_6$ ,  $\text{ClO}_4$ ...] Bechgaard salts have become the prototypical examples of quasi-one-dimensional (Q1D) conductors with the highest conductivity direction parallel to the stacking axis ( $\mathbf{a}$ ) of the TMTSF molecules. Their low temperature properties have attracted much attention since various transitions such as incommensurate spin-density-wave (SDW), superconductivity, field-induced SDW, quantum Hall effect etc., have been observed [1]. Recently, the normal phase (*i.e.* above the transition temperature of the broken symmetry ground states) has attracted much interest. Since the tunneling integral along the chain direction ( $t_a \sim 0.25$  eV) is at least one order of magnitude larger than the transfer integrals  $t_b$  and  $t_c$  in the transverse directions ( $t_b \sim 200$  K and  $t_c \sim 10$  K), the organic metallic chains are usually considered as weakly coupled. Although the coupling along  $\mathbf{c}$  is likely irrelevant over a large temperature domain, the effective value of  $t_b$  has to be considered to precise the dimensionality of the electron gas in the normal phase. At sufficiently high temperatures however, the physical properties are expected to be essentially governed by 1D phenomena.

It is well known that, in a strictly 1D interacting electron gas, the Fermi liquid (FL) picture breaks down and must be replaced by the so-called Luttinger liquid (LL) description [2]. Since non-negligible interchain coupling along the  $\mathbf{b}'$  direction exist in the Bechgaard's salts, departure from the LL model [3] might be induced. Indeed, when the temperature is progressively lowered, transverse  $\mathbf{b}'$  interactions are expected to become more effective so that a crossover from a Q1D to a two-dimensional (2D) electron gas picture should occur: the FL behavior might be recovered provided that the Coulomb interactions are not too strong. However, the actual value of the crossover temperature  $T_x$  is highly debated. According to simple band calculations, the dimensional crossover for the single particle motion is then expected to occur at  $T_x \sim 150 - 200$  K. This is in agreement with the temperature dependence of the longitudinal DC resistivity which is showing a transition regime from a roughly linear behavior to a  $T^2$  profile (indicative of a FL behavior dominated by electron-electron scattering effects) over that temperature range [4]. However, photoemission spectra [5,6] are incompatible with a FL picture over that temperature range and early optical experiments with the light polarized along the transverse  $\mathbf{b}'$  direction failed to evidence a coherent plasma edge above 50 K [7]. Moreover, deviations from the FL picture have also been observed down to 50 K in NMR experiments, suggesting then an upper bound value for the crossover temperature

---

<sup>a</sup> Present address: LCM3B, Université Henri Poincaré, Nancy I, BP 239, 54 506 Vandoeuvre-les-Nancy Cedex, France  
e-mail: pfertey@lcm3b.u-nancy.fr

[8,9]. Furthermore, the frequency dependence of the conductivity is well known to display unusual features [10,11]: for frequencies above the effective interchain transfer integral, the electrodynamics is consistent with the prediction of the LL picture, while at low frequencies, pronounced deviations with respect to the Drude picture are present [12].

Among all the experimental approaches used to study the dimensionality of the electron gas, transverse transport measurements are particularly relevant to directly probe the interchain couplings. It was further realized that since the transverse transfer integrals are small, an electric field applied along the  $\mathbf{b}'$  or  $\mathbf{c}^*$  directions could also act as a probe of the physical properties in the plane perpendicular to that direction. Early resistivity measurements [13] along the hard axis ( $\mathbf{c}^*$ ) have shown a non monotonic behavior of the temperature profile: a maximum of  $\rho_c$  was observed near 80 K. More recently, a strong pressure dependence of this unusual feature was evidenced [14] and a typical 1D power law profile was found above the characteristic  $\rho_c$  maximum. This maximum was then ascribed to a broad crossover regime indicative of a deconfinement of the carriers from the chain axis; this results in a gradual onset of coherent transport along  $\mathbf{b}'$  below 80 K, suggesting then a FL behavior in the  $\mathbf{a}$ - $\mathbf{b}'$  plane. However, the anisotropy ratio  $\rho_c/\rho_a$  was not found temperature independent as expected from FL arguments and an incipient Fermi liquid was therefore invoked. These observations contrast with the work of Gor'kov *et al.* [15–17] who recently argued that the longitudinal transport properties, below 60 K and down to the SDW transition temperature, can be well accounted for in terms of a weakly interacting Fermi liquid. However, such a quasi-particle like signature (if ever) should also be detected in the  $\mathbf{b}'$  transverse direction.

Reliable measurements of the transverse transport properties along  $\mathbf{b}'$  are highly needed to clarify the present controversy. Unfortunately, since the Bechgaard salts have a pronounced needle shape whose axis is parallel to the chains, transverse transport along  $\mathbf{b}'$  is particularly difficult to perform with usual DC methods. Owing to non-uniform current distributions between contacts, parasitic contributions from other directions are likely introduced. These problems can be avoided by using a contactless microwave technique which allows a better control on the orientation of the current lines in these organic needles. In this paper, we report microwave resistivity data obtained along the transverse directions in  $(\text{TMTSF})_2\text{PF}_6$  crystals. These data clearly indicates the temperature range over which the coherence of interchain hopping sets in and they confirm strong deviations from a Fermi liquid description.

## 2 Experiment

High quality single crystals of  $(\text{TMTSF})_2\text{PF}_6$  have been synthesized by the standard electrochemical method with typical dimensions ( $\sim 8 \times 0.25 \times 0.1 \text{ mm}^3$ ) along the  $\mathbf{a}$ ,  $\mathbf{b}'$  and  $\mathbf{c}^*$  axes respectively. Such a needle geometry is not

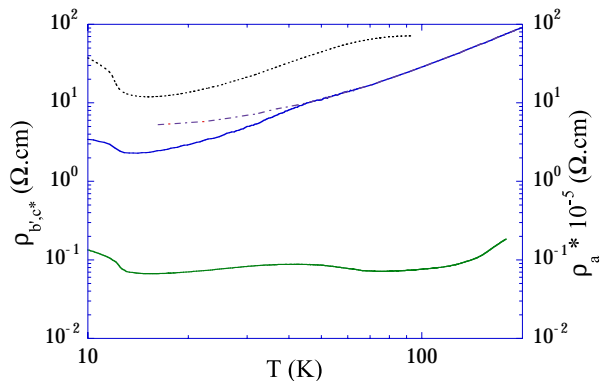


**Fig. 1.** Microwave resistivity of  $(\text{TMTSF})_2\text{PF}_6$  as a function of temperature along  $\mathbf{a}$  (full),  $\mathbf{b}'$  (dashed) and  $\mathbf{c}^*$  (dotted) axes. The dashed-dotted line mimics the behavior of the dc resistivity along the chain axis.

suitable for precise measurement of the transverse transport properties; this is particularly true for our microwave technique which yields very accurate data only when the electric field is oriented along the needle's axis. Each needle was therefore cut into three pieces in order to perform the measurements along the  $\mathbf{a}$ ,  $\mathbf{b}'$  and  $\mathbf{c}^*$  axes (natural faces of the single crystals) on the same single crystal. Each piece was then cut in small blocks so that it could be reconstructed with the shape of a needle having one of the crystal directions as its axis. We used a conventional cavity perturbation technique at 16.5 GHz [18] to obtain the electrical resistivity along each crystal axes as a function of the temperature (2-300 K) and a magnetic field (0-14 T) applied along the  $\mathbf{c}^*$  direction. Unfortunately, due to the microwave resonator design, no data could be collected with both the magnetic field and the electric field along the  $\mathbf{c}^*$  axis. To prevent microcracks the samples were slowly cooled to the lowest temperature at 0.6 K/min. The temperature was monitored either with a Si diode (zero field) or a capacitor sensor (field up to 14 T).

## 3 Results and discussion

Along the high conductivity axis, the microwave resistivity has been determined by using the Hagen-Rubens limit (skin depth regime). Since the conductivity is much lower along the  $\mathbf{b}'$  and  $\mathbf{c}^*$  axes, the microwave data were rather analyzed in the framework of the metallic limit of the quasistatic approximation [19]. We report in Figure 1, the temperature profile of the resistivity along the ( $\mathbf{a}$ ), ( $\mathbf{b}'$ ) and ( $\mathbf{c}^*$ ) axes of  $(\text{TMTSF})_2\text{PF}_6$  in the normal phase for zero magnetic field value. The orders of magnitude are in good agreement with published DC results [13,14] and the SDW phase is evidenced for each crystal direction by an abrupt resistivity increase below 12 K.

Along the chain axis ( $\mathbf{a}$ ), the usual metallic behavior is observed down to 13.6 K, where the resistivity reaches a minimum. Interestingly, the microwave resistivity profile

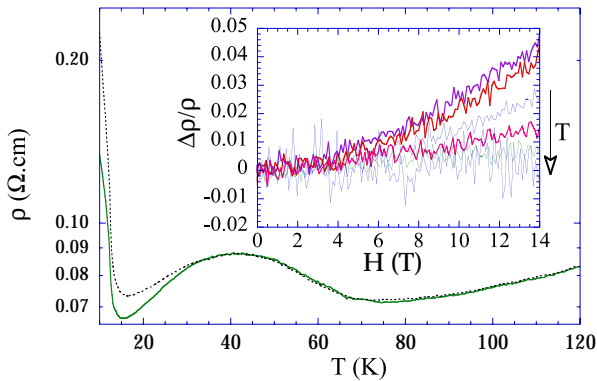


**Fig. 2.** Microwave resistivity along  $\mathbf{b}'$ , in zero (full) and 14 T (dotted) magnetic field values. Inset: relative magnetoconductivity measured at 16, 18, 20, 25, 35 and 80 K. The right arrow indicates the temperature variation.

displays clearly, near 45 K, a change of slope, when the DC one usually shows a single quadratic behavior below 100 K (dashed-dotted line in Fig. 1). Along the least conducting direction ( $\mathbf{c}^*$ ), the microwave resistivity profile is consistent with the DC curve [14]: it increases first when the temperature is decreased from 300 K (not shown on the figure), reaches a maximum near 90 K and recovers a metallic behavior on further cooling. The minimum value is obtained near 15.3 K. The  $\mathbf{b}'$  resistivity presents definitely a different profile, being almost flat (below 120 K) on the logarithmic scale compared to the other crystal directions. This profile is shown in more details in Figure 2. On lowering the temperature, the resistivity  $\rho_{b'}$  first decreases monotonically down to a local minimum around 75 K, increases slightly to reach a local maximum near 40 K and decreases again down to 15 K before entering the SDW phase below 12 K. This peculiar profile observed between 12 and 80 K is weakly sample dependent: this is illustrated in Figure 3 where we compare the normalized resistivity (relative to the value just above the SDW transition) obtained on three different samples (different batches). Such a dependency can be explained by two factors: (i) a slight misalignment relative to one another of the small crystals used in the needle's construction; (ii) a different impurity content in crystals of different batches. A correlation with the latter factor is difficult to evaluate for the moment. However, it seems clear from Figure 3 that the local maximum of  $\rho_{b'}$  around 40 K is intrinsic to this crystal direction. Its absence on the DC resistivity profile [13] could signify that the latter is significantly polluted by different components of the resistivity tensor as previously mentioned.

The emergence of an insulating behavior below 70 K ( $d\rho_{b'}/dT < 0$  in Fig. 2) refutes the possible existence of quasi-particle states down to 40 K. A Fermi liquid description of interacting electrons above 40 K would, indeed, have required a quadratic temperature profile of both the  $\rho_a$  and  $\rho_{b'}$  components. Between 50 K and 70 K,  $\rho_{b'}$  is better understood by assuming a Luttinger liquid be-

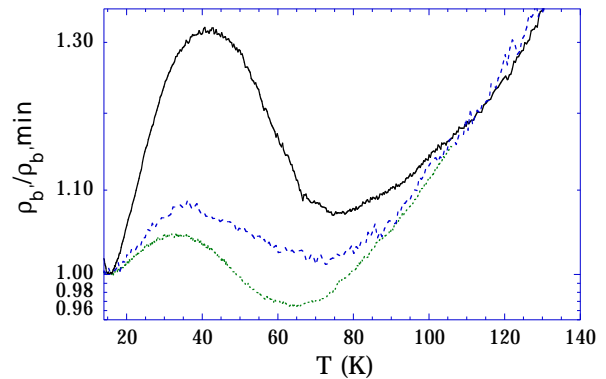


**Fig. 3.** Sample effect on  $\rho_{b'}$  at intermediate temperatures for sample 1 (full), 2 (dashed) and 3 (dotted).

havior along the stacks: this yields a power-law increase  $\rho_{b'}(T) \sim T^{-2\alpha}$ , where  $\alpha$  is the exponent of the single-particle density of states of the LL [14]. However, due to the reduced temperature domain used to fit the power law and the slight sample dependency of  $\rho_{b'}$  in this temperature range, the exponent  $\alpha$  might be only approximative ( $2\alpha \sim 0.3$ ) and prevent in turn reliable determination value of the exponent  $K_\rho$  characterizing the charge degrees of freedom of a LL.

The resistivity maximum observed around 40 K could therefore be attributed to the onset of a deconfinement of the carriers and the restoration of a 2D conductivity regime in the  $\mathbf{a-b}$  plane below 40 K. This is supported by the observation of an important increase of the resistivity when a magnetic field is applied perpendicularly to the 2D plane of motion (Fig. 2), only for temperatures below 40 K. This is exemplified in the inset of Figure 2 which displays the variation of the resistivity relatively to its zero field value as a function of the magnetic field for temperatures between 16 and 80 K. It is well known that in the Bechgaard salts, a magnetic field applied along the hard axis  $\mathbf{c}^*$  confines the motion of the carriers to the chain axis. Therefore, a reduction of the metallic behavior parallel to  $\mathbf{b}'$  is expected if there is some coherent motion along that direction. Below 40 K, the progressively increasing magnetoconductivity can then be interpreted as the signature of the 2D motion. On the contrary, since no magnetoconductivity is observed above 40 K, transverse coherent hopping is apparently absent and coherent motion is confined to the organic stacks. This observation of a dimensional crossover around 40 K supports the predictions of the renormalization group theory: a Luttinger liquid picture may persist down to the low temperature region when many-body effects on interchain hopping are considered [20]. Indeed, one-dimensional many-body effects are expected to lower the efficiency of interchain tunneling, thereby decreasing its amplitude. However, transient effects are likely associated to such a crossover since the deconfinement region is not sharply defined but spread out in temperature: in the coherent regime (16-30 K),  $\rho_{b'}$  does not show a quadratic temperature profile (the power law

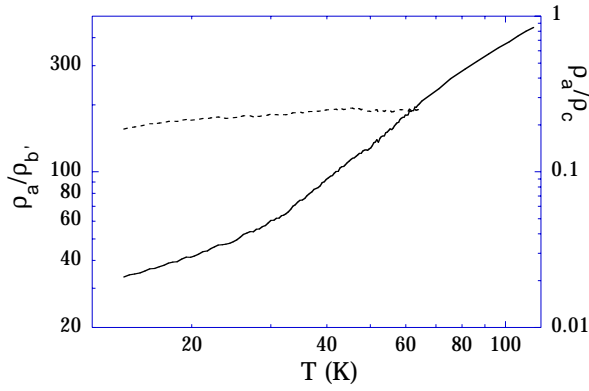


**Fig. 4.** Temperature profiles of the anisotropy ratios  $\rho_a/\rho_{b'}$  (line) and  $\rho_a/\rho_{c^*}$  (dashed).

exponent ranges from 0.37 to 0.075 for the three samples studied). This signifies that important deviations from a FL quasi-particle transport exist along the  $\mathbf{b}'$  axis, as exemplified by the temperature profile of the microwave resistivity anisotropy ratio  $\rho_a/\rho_{b'}$  and  $\rho_a/\rho_{c^*}$  presented in Figure 4.

Below 70 K,  $\rho_a/\rho_{c^*}$  is practically constant: it can be reasonably fitted by a  $\sim T^{0.15}$  law in clear contrast with the results of Moser *et al.* [14], ( $\sim T^{0.5}$ ) over the same temperature range. On the contrary,  $\rho_a/\rho_{b'}$  continuously decreases from 300 K down to the SDW transition temperature. Only a change of curvature is observed around the dimensional crossover temperature near 40 K, seemingly in contradiction with a constant ratio expected for a true FL behavior.

The onset of coherence transport along the transverse direction is also supported by some features observed on the microwave resistivity along the chain axis. We show, in Figure 5, a significant increase of the resistivity for a magnetic field of 14 T applied along  $\mathbf{c}^*$ . As seen in the inset, a significant magnetoresistance is again observed only for temperatures below 40 K, consistently with a dimensional crossover over that range. The change of slope precedingly identified on  $\rho_a$  around 45 K in zero field thus signals the onset of transverse coherent transport.

However, the temperature scale of the deconfinement deduced from microwave measurements along the  $\mathbf{b}'$  direction is a factor of two smaller than the one deduced by Moser *et al.* from DC resistivity along the hard axis  $\mathbf{c}^*$  [14], a feature also seen in Figure 1. The reason for this is unclear at the moment but the discrepancy between the results for both directions may indicate that probing the  $\mathbf{ab}$  plane through  $\rho_c$  is less accurate in the extraction of the electronic transport along the  $\mathbf{b}$  direction.

## 4 Conclusion

The microwave resistivity data reported in this paper for  $(\text{TMTSF})_2\text{PF}_6$  crystals clearly show the onset of coherent transport properties along the intermediate conductivity

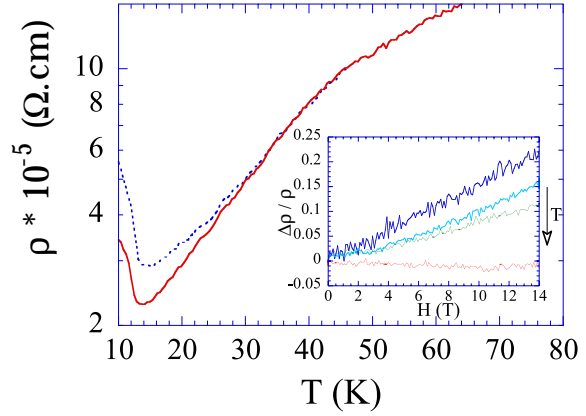


**Fig. 5.** Temperature profile of the chain axis microwave resistivity in zero (full) and 14 T (dotted) magnetic field values. Inset: relative magnetoresistance measured at 14, 16, 18 and 80 K. The right arrow indicates the temperature variation.

direction  $\mathbf{b}'$  below about 40 K. This temperature scale is evidenced by a resistivity maximum around 40 K along the  $\mathbf{b}'$  axis and supported by a progressively increasing magnetoresistance below 40 K, when a magnetic field is applied along  $\mathbf{c}^*$ . Similar effects observed on the temperature profile of the longitudinal resistivity  $\rho_a$  confirm the dimensional crossover. Furthermore, a temperature profile analysis of  $\rho_{b'}$  has failed to detect any clear-cut Fermi liquid component in the whole normal phase domain, in good agreement with previous results such as NMR [8,9], photoemission [5] or optical data [12], though the anisotropy ratio deduced from reflectance analysis [10,11] seems surprisingly well described by band parameters. A detailed theoretical framework that would clarify why some experimental probes are apparently strongly sensitive to many-body effect while others do not, is missing so far.

The authors are grateful to J. Beerens for giving access to his 14 T experimental set-up, to C. Bourbonnais for critical reading of the manuscript and useful suggestions during the course of this work, M. Castonguay and J. Corbin for technical assistance. This work was supported by grants from the Fonds pour la Formation de Chercheurs et l'Aide à la Recherche of the Government of Québec (FCAR) and from the Natural Science and Engineering Research Council of Canada (NSERC).

## References

1. T. Ishiguro, K. Yamaji, in *Organic Superconductors*, edited by P. Fulde (Springer-Verlag, Berlin, 1990).
2. H.J. Schulz, *Int. J. Mod. Phys. B* **5**, 57 (1991).
3. see *e.g.* D. Boies, C. Bourbonnais, A.-M.S. Tremblay, *Phys. Rev. Lett.* **74**, 968 (1995) and references therein.
4. D. Jérôme, in *Organic Superconductors*, edited by J.P. Farges (Marcel Dekker, New York, 1994), p 405.

5. B. Dardel, D. Malterre, M. Grioni, P. Weibel, Y. Baer, J. Voit, D. Jérôme, *Europhys. Lett.* **24**, 687 (1993).
6. F. Zwick, S. Brown, G. Margaritondo, C. Merlic, M. Onellion, J. Voit, M. Grioni, *Phys. Rev. Lett.* **79**, 3982 (1997).
7. C.S. Jacobsen, D.B. Tanner, K. Bechgaard, *Phys. Rev. B* **28**, 7019 (1983).
8. C. Bourbonnais, *J. Phys. I France* **3**, 143 (1993).
9. P. Wzietek, F. Creuzet, C. Bourbonnais, D. Jérôme, K. Bechgaard, P. Batail, *J. Phys. I France* **3**, 171 (1993).
10. A. Schwartz, M. Dressel, G. Grüner, V. Vescoli, L. Degiorgi, T. Giamarchi, *Phys. Rev. B* **58**, 1261 (1998).
11. V. Vescoli, L. Degiorgi, W. Henderson, G. Grüner, K.P. Sarkey, L.K. Montgomery, *Science* **281**, 1181 (1998).
12. N. Cao, T. Timusk, K. Bechgaard, *J. Phys. I France* **6**, 1719 (1996).
13. C.S. Jacobsen, K. Mortensen, M. Weger, K. Bechgaard, *Sol. State Comm.* **38**, 423 (1981).
14. J. Moser, M. Gabay, P. Auban-Senzier, D. Jérôme, K. Bechgaard, J.M. Fabre, *Euro. Phys. J. B* **1**, 39 (1998).
15. L.P. Gor'kov, M. Mochena, *Phys. Rev. B* **57**, 6204 (1998).
16. L.P. Gor'kov, *J. Phys. I France* **6**, 1697 (1996).
17. L.P. Gor'kov, *Europhys. Lett.* **31**, 49 (1995).
18. P. Fertey, M. Poirier, H. Muller, *Phys. Rev. B* **57**, 14357 (1998).
19. J.L. Musfeldt, M. Poirier, P. Batail, C. Lenoir, *Phys. Rev. B* **51**, 8347 (1995) and references therein.
20. C. Bourbonnais, *Mol. Cryst. Liq. Cryst.* **119**, 11 (1985).